Three Different Continuous-Time GMDS-ZNN Models and Multiple-Instant Discrete-Time Ones for Time-Varying Matrix Inversion with Comparisons

Kangze Zheng*, Yunong Zhang*
*School of Computer Science and Engineering, Sun Yat-sen University, Guangzhou 510006, P. R. China
zhengkz@mail2.sysu.edu.cn, zhynong@mail.sysu.edu.cn

2021 China Automation Congress (CAC) | 978-1-6654-2647-3/21/$31.00 ©2021 IEEE | DOI: 10.1109/CAC53003.2021.9728668

***Abstract*—Securing the inverse matrix of a matrix varied with time online plays a considerable role in many engineering and scientific applications. Lots of effort has been made in securing the inverse varied with time of an interesting matrix with high speed and high accuracy so far. With the rapid development of neural networks and neural-dynamic methods, Getz-Marsden dynamic system (GMDS) is propounded to secure the time-varying matrix inversion. Subsequently, Zhang *et al.* put forward Zhang neural network (ZNN, also zeroing neural network as termed) models and Zhang functions (ZFs, also termed zeroing functions), with several kinds of GMDS-ZNN (GZ) models constructed in real and complex domains by means of ZNN models and ZFs. In the meantime, many researches on the features of these GZ models are carried out. However, there is no comparison among these GZ models. Hence, we conduct numerical experiments to compare three GZ models, including GZ model 1 (also termed GMDS), GZ model 2, and GZ model 3. The results of numerical computer experiments substantiate that GZ model 2 and 3 are evidently better in two aspects (i.e., convergence accuracy and convergence rate), compared with GZ model 1. Besides, the numerical results synthesized by GZ model 2 are completely the same as those synthesized by GZ model 3.**

***Index Terms*—online time-varying matrix inversion, GMDS-ZNN models, time-discretization formulas, comparisons, performance**

I. Introduction

Recently, the quite tough issue of how to secure time-varying continuous or discrete matrix inversion online comes into notice frequently in distinct categories of engineering and scientific applications, like robotics control [1], [2], optimization [3] , machine learning [4], and image restoration [5], [6]. Evidently, it is pretty significant to solve this problem fast and accurately. Therefore, a host of researches have been carried out to solve it. However, the serial-processing algorithms, which were put forward at the beginning, are less efficient when confronting large-scale online applications. This is because their minimal computational complexities are in proportion to the cubic of the dimension of the interesting matrix, which implies that the serial-processing algorithms are less capable of meeting the requirement of computation speed in online applications [7], [8]. Inevitably, to expedite computation speed, parallel-processing algorithms are proposed. Lately, neural-dynamic methods (e.g., neuronets, i.e., neural networks) have been extensively employed and acknowledged as an excellent approach to settling the issue of the time-varying matrix inversion, on account of their striking merits such as the capability of swift parallel-type processing distribution-type storage, the simplicity of basic hardware realization, and the outstanding performance in online large-scale practice [3], [8]–[11] . Furthermore, with the gradual progress of neural networks, Zhang and his coworkers have propounded and investigated a novel category of recurrent neural networks, known as ZNN (Zhang neuronet or Zhang neural network as termed), to secure the inverse varied with time of an interesting matrix [12]. So far, ZNN has been applied to the robotics kinematics [13] , the nonlinear time-varying equation systems [14], and the matrix inversion varied with time [5]. Besides, the Zhang function (ZF), an indefinite error function, is the core of ZNN [5].

In 1997, Getz and Marsden proposed Getz-Marsden dynamic system (GMDS) that is utilized for the time-varying matrix inversion [15]. Furthermore, Zhang *et al.* presented GMDS-ZNN (GZ) model 1 [5], GZ model 2 [8], and GZ model 3 [16], simply and collectively, GZ neural dynamics (GZND) models, by adopting the tools of ZF, ZNN design formula, and gradient dynamic system (GDS) design. It should be noted that both GZ model 2 and 3 possess the advantages of both ZNN and GDS. In addition, two GMDS variants were raised in [17]. On account of digital hardware implementation, the majority of continuous-time models should be discretized [18]. From preceding researches [8], [15]–[17], [19], [20], it is evident that continuous GZ models are expressed in the form of differential (more rigorously, derivative, also termed differential-quotient) equations. A class of ZTD (Zhang time discretization as termed) [21]–[29] , being a part of numerical differentiation, which approximates the 1-st order derivative of a certain function with regard to time at a certain time instant, based on the values of the function at the present and previous instants, is a feasible approach to the time discretization of GDMS-ZNN models. Hitherto, a number of time-discretization formulas have been constructed and exploited. Note that the precision of a time-discretization formula influences the accuracy of the obtained discrete model. To be precise, the more precise a time-discretization formula is, the smaller the error of the corresponding discrete model is. According to previous work [8], [15]–[17], [19], [20], numerous characteristics of the above continuous-time models have been discovered and studied. However, there is no comparison among GZ model 1, 2, and 3, especially, in discrete

time. Thus, we carry out numerical computer experiments for comparisons. Here are the relatively major contributions of the paper.

- We illustrate the design procedures of three continuous-time GZ models in detail.
- Through experiments and comparisons, it is discovered that GZ model 2 or 3 performs better than GZ model 1.
- We figure out that, when exploiting the same time-discretization formula, the results of GZ model 2 are totally the same as those of GZ model 3, regardless of whether the experimental subject is a real time-varying matrix or a complex time-varying one. In addition, different discrete-time GZ models have their own precisions related to the exploited time-discretization formulas, which is distinguished from GZ variants.

The are four sections as the remainder of our paper. Section II presents mathematical formulation for the issue of the time-varying matrix inversion, as well as the design procedures of three GZ models. In Section III, we utilize five time-discretization formulas to discretize GZ models, including Euler forward formula (EFF), Zhang-Taylor (ZT) discretization formula (constructed by Taylor expansion [21]) as a part of ZTD, a 6-instant ZTD formula, and two 8-instant ZTD formulas. In Section IV, for comparisons, two examples' numerical experiments are provided, and Section V sums up our paper.

II. Mathematical Formulation and Continuous-Time GZ Models

This section presents the mathematical formulation for the issue of the time-varying matrix inversion. Additionally, continuous-time GZ models are elaborated.

A. Mathematical Formulation for Problem

The formulation for the time-varying matrix inversion issue is expressed as

$$C(t)M(t) = I, \tag{1}$$

in which $C(t) \in \mathbb{C}^{n\times n}$ is a smooth and nonsingular matrix varied with time, $M(t) \in \mathbb{C}^{n\times n}$ is to be online solved for, and $I \in \mathbb{R}^{n\times n}$ is the identity matrix. It should be pointed out that the matrix $M(t)$ obtained in problem (1), is in a discrete-time modality, namely $M(t = k\tau)$ with $k \in \mathbb{N}$ and $\tau \in \mathbb{R}^+$ denoting the sampling interval.

B. GZ Model 1

First, we define an error function whose value is a matrix [5]:

$$E(t) = C(t) - M^{-1}(t) \in \mathbb{C}^{n\times n},$$

which is actually a ZF, to supervise and regulate the solving process of problem (1). Second, via employing $\dot{E}(t) = -\lambda E(t)$ (a design formula proposed by Zhang and his coworkers [5]), an equation is acquired as

$$\dot{C}(t) + M^{-1}(t)\dot{C}(t)M^{-1}(t) = -\lambda\left(C(t) - M^{-1}(t)\right).$$

Third, by rearranging the above equation, GZ model 1 is presented as [5]:

$$\dot{M}(t) = -M(t)\dot{C}(t)M(t) - \lambda M(t)\left(C(t)M(t) - I\right), \tag{2}$$

where $\lambda \in \mathbb{R}^+$ is a design parameter for scaling convergence rate.

C. GZ Model 2

The second GZ model is derived from the subtle combination of GZ model 1 (2) and GDS. According to [8], we design a nonnegative function : $\epsilon(t) = \|C(t)M(t) - I\|_{\mathrm{F}}^2/2 \in \mathbb{R}$, namely the square of the Frobenius norm of $C(t)M(t) - I$. Evidently, $\epsilon(t)$ approaches 0 as $M(t)$ approaches $C^{-1}(t)$ with $t \to +\infty$. Furthermore, we acquire a GDS for problem (1) as follows:

$$\dot{M}(t) = -\lambda\frac{\partial\epsilon(t)}{\partial M(t)} = -\lambda C^{\mathrm{H}}(t)\left(C(t)M(t) - I\right), \tag{3}$$

in which $C^{\mathrm{H}}(t)$ represents the conjugate transpose matrix of $C(t)$. By substituting the ZNN error feedback of (2), namely $-\lambda M(t)\left(C(t)M(t) - I\right)$, with the GDS error feedback of (3), namely $-\lambda C^{\mathrm{H}}(t)\left(C(t)M(t) - I\right)$, GZ model 2 is presented as

$$\dot{M}(t) = -M(t)\dot{C}(t)M(t) - \lambda C^{\mathrm{H}}(t)\left(C(t)M(t) - I\right). \tag{4}$$

Through a host of practice, it is discovered that the convergence accuracy of ZNN is high and the convergence rate of GDS is fast. Furthermore, GZ model 2 depicted in (4) has the strengths of both ZNN and GDS.

D. GZ Model 3

The design procedure of the third GZ model resembles that of the second GZ model depicted in (4). The difference is the nonnegative scalar-valued energy function which we define, that is, $\epsilon(t) = \|M(t)C(t) - I\|_{\mathrm{F}}^2/2 \in \mathbb{R}$. Thereby, we have another GDS for problem (1) [16]:

$$\dot{M}(t) = -\lambda\frac{\partial\epsilon(t)}{\partial M(t)} = -\lambda\left(M(t)C(t) - I\right)C^{\mathrm{H}}(t). \tag{5}$$

Similarly, substitute the ZNN error feedback of (2), namely $-\lambda M(t)\left(C(t)M(t) - I\right)$, with the GDS error feedback of (5), namely $-\lambda\left(M(t)C(t) - I\right)C^{\mathrm{H}}(t)$. Then, GZ model 3 is formulated as follows:

$$\dot{M}(t) = -M(t)\dot{C}(t)M(t) - \lambda\left(M(t)C(t) - I\right)C^{\mathrm{H}}(t). \tag{6}$$

In the same way, GZ model 3 depicted in (6) acquires the advantages of both ZNN and GDS.

III. Discrete-Time GZ Models

Due to digital hardware implementation, we should discretize the above models to investigate their characteristics. In this section, we apply five different time-discretization formulas (i.e., EFF, ZT discretization formula, one ZTD formula with 6 instants, and two ZTD formulas with 8 instants) to discretize the above GZ models.

A. EFF and Corresponding Models

EFF, which has been put forward for more than two hundred years, is a simple but brilliant method for numerically solving ordinary derivative equations (ODE) [30], [31]. EFF is expressed as

$$\dot{M}_k = \frac{1}{\tau}(M_{k+1} - M_k) + O(\tau),$$

where $k \in \mathbb{N}$ denotes the index, and $\tau \in \mathbb{R}^+$ denotes the sampling interval. Via replacing $\dot{M}(t)$ in (2), (4), and (6), three discrete GZ models discretized by EFF are shown as follows:

$$M_{k+1} \doteq -\tau M_k \dot{C}_k M_k - hM_k(C_k M_k - I) + M_k, \tag{7}$$

$$M_{k+1} \doteq -\tau M_k \dot{C}_k M_k - hC_k^{\mathrm{H}}(C_k M_k - I) + M_k, \tag{8}$$

and

$$M_{k+1} \doteq -\tau M_k \dot{C}_k M_k - h(M_k C_k - I)C_k^{\mathrm{H}} + M_k, \tag{9}$$

where $\doteq$ denotes the computational assignment operator, $h = \lambda\tau \in \mathbb{R}^+$ represents the step size. We name (7), (8), and (9) as DTGZ1-I, DTGZ2-I, and DTGZ3-I, respectively.

B. ZT Discretization Formula and Corresponding Models

ZT discretization formula, which has been proposed since 2014, fixes a few natural defects of both the backward numerical differentiation and the central one [21], [32]. Besides, the shortcoming of the Lagrange interpolation formula is overcome by ZT discretization formula which is formulated as [21], [32]:

$$\dot{M}_k = \frac{1}{2\tau}(2M_{k+1} - 3M_k + 2M_{k-1} - M_{k-2}) + O(\tau^2).$$

By replacing $\dot{M}(t)$ in (2), (4), and (6), the discrete-time GZ models discretized by ZT discretization formula are shown as follows:

$$\begin{aligned} M_{k+1} \doteq &-\tau M_k \dot{C}_k M_k - hM_k(C_k M_k - I) + \frac{3}{2}M_k \\ &- M_{k-1} + \frac{1}{2}M_{k-2}, \end{aligned} \tag{10}$$

$$\begin{aligned} M_{k+1} \doteq &-\tau M_k \dot{C}_k M_k - hC_k^{\mathrm{H}}(C_k M_k - I) + \frac{3}{2}M_k \\ &- M_{k-1} + \frac{1}{2}M_{k-2}, \end{aligned} \tag{11}$$

and

$$\begin{aligned} M_{k+1} \doteq &-\tau M_k \dot{C}_k M_k - h(M_k C_k - I)C_k^{\mathrm{H}} + \frac{3}{2}M_k \\ &- M_{k-1} + \frac{1}{2}M_{k-2}. \end{aligned} \tag{12}$$

We name (10), (11), and (12) as DTGZ1-II, DTGZ2-II, and DTGZ3-II, respectively.

C. 6-Instant ZTD Formula and Corresponding Models

Compared with ZT discretization formula, the highest precision of 6-instant ZTD formulas is higher. According to the previous work [33], [34], a specific ZTD formula with 6 instants is expressed as

$$\begin{aligned} \dot{M}_k = &\frac{1}{42\tau}(23M_{k+1} - 11M_k - 4M_{k-1} - 5M_{k-2} \\ &- 7M_{k-3} + 4M_{k-4}) + O(\tau^3). \end{aligned}$$

By replacing $\dot{M}(t)$ in (2), (4), and (6), the discrete-time GZ models discretized by the 6-instant ZTD formula are shown as follows:

$$\begin{aligned} M_{k+1} \doteq &-\frac{42}{23}\tau M_k \dot{C}_k M_k - \frac{42}{23}hM_k(C_k M_k - I) + \frac{11}{23}M_k \\ &+ \frac{4}{23}M_{k-1} + \frac{5}{23}M_{k-2} + \frac{7}{23}M_{k-3} - \frac{4}{23}M_{k-4}, \end{aligned} \tag{13}$$

$$\begin{aligned} M_{k+1} \doteq &-\frac{42}{23}\tau M_k \dot{C}_k M_k - \frac{42}{23}hC_k^{\mathrm{H}}(C_k M_k - I) + \frac{11}{23}M_k \\ &+ \frac{4}{23}M_{k-1} + \frac{5}{23}M_{k-2} + \frac{7}{23}M_{k-3} - \frac{4}{23}M_{k-4}, \end{aligned} \tag{14}$$

and

$$\begin{aligned} M_{k+1} \doteq &-\frac{42}{23}\tau M_k \dot{C}_k M_k - \frac{42}{23}h(M_k C_k - I)C_k^{\mathrm{H}} + \frac{11}{23}M_k \\ &+ \frac{4}{23}M_{k-1} + \frac{5}{23}M_{k-2} + \frac{7}{23}M_{k-3} - \frac{4}{23}M_{k-4}. \end{aligned} \tag{15}$$

We name (13), (14), and (15) as DTGZ1-III, DTGZ2-III, and DTGZ3-III, respectively.

D. 8-Instant ZTD Formulas and Corresponding Models

According to the previous work [35], [36], two specific 8-instant ZTD formulas with higher precision are presented as

$$\begin{aligned} \dot{M}_k = &\frac{1}{2220\tau}(1000M_{k+1} - 51M_k - 400M_{k-1} - 600M_{k-2} \\ &- 200M_{k-3} + 175M_{k-4} + 176M_{k-5} - 100M_{k-6}) \\ &+ O(\tau^4) \end{aligned} \tag{16}$$

and

$$\begin{aligned} \dot{M}_k = &\frac{1}{72\tau}(31M_{k+1} + 3M_k - 16M_{k-1} - 24M_{k-2} - M_{k-3} \\ &+ 7M_{k-4} + 2M_{k-5} - 2M_{k-6}) + O(\tau^4). \end{aligned} \tag{17}$$

By replacing $\dot{M}(t)$ in (2), (4), and (6), the discrete-time GZ models discretized by (16) are shown as follows:

$$\begin{aligned} M_{k+1} \doteq &-\frac{111}{50}\tau M_k \dot{C}_k M_k - \frac{111}{50}hM_k(C_k M_k - I) \\ &+ \frac{51}{1000}M_k + \frac{2}{5}M_{k-1} + \frac{3}{5}M_{k-2} + \frac{1}{5}M_{k-3} \\ &- \frac{7}{40}M_{k-4} - \frac{22}{125}M_{k-5} + \frac{1}{10}M_{k-6}, \end{aligned} \tag{18}$$

$$\begin{aligned} M_{k+1} \doteq &-\frac{111}{50}\tau M_k \dot{C}_k M_k - \frac{111}{50}hC_k^{\mathrm{H}}(C_k M_k - I) \\ &+ \frac{51}{1000}M_k + \frac{2}{5}M_{k-1} + \frac{3}{5}M_{k-2} + \frac{1}{5}M_{k-3} \\ &- \frac{7}{40}M_{k-4} - \frac{22}{125}M_{k-5} + \frac{1}{10}M_{k-6}, \end{aligned} \tag{19}$$

TABLE I: Expressions of continuous and corresponding discrete GZ models

Model	Expressions	
	Continuous-time model expression	**Discrete-time model expressions**
GZ model 1	$\dot{M}(t) = -M(t)\dot{C}(t)M(t) - \lambda M(t)\left(C(t)M(t) - I\right)$	$M_{k+1} \doteq -\tau M_k \dot{C}_k M_k - hM_k(C_k M_k - I) + M_k$ $M_{k+1} \doteq -\tau M_k \dot{C}_k M_k - hM_k(C_k M_k - I) + \frac{3}{2}M_k$ $-M_{k-1} + \frac{1}{2}M_{k-2}$ $M_{k+1} \doteq -\frac{42}{23}\tau M_k \dot{C}_k M_k - \frac{42}{23}hM_k(C_k M_k - I)$ $+\frac{11}{23}M_k + \frac{4}{23}M_{k-1} + \frac{5}{23}M_{k-2}$ $+\frac{7}{23}M_{k-3} - \frac{4}{23}M_{k-4}$ $M_{k+1} \doteq -\frac{111}{50}\tau M_k \dot{C}_k M_k - \frac{111}{50}hM_k(C_k M_k - I)$ $+\frac{51}{1000}M_k + \frac{2}{5}M_{k-1} + \frac{3}{5}M_{k-2} + \frac{1}{5}M_{k-3}$ $-\frac{7}{40}M_{k-4} - \frac{22}{125}M_{k-5} + \frac{1}{10}M_{k-6}$ $M_{k+1} \doteq -\frac{72}{31}\tau M_k \dot{C}_k M_k - \frac{72}{31}hM_k(C_k M_k - I)$ $-\frac{3}{31}M_k + \frac{16}{31}M_{k-1} + \frac{24}{31}M_{k-2} + \frac{1}{31}M_{k-3}$ $-\frac{7}{31}M_{k-4} - \frac{2}{31}M_{k-5} + \frac{2}{31}M_{k-6}$
GZ model 2	$\dot{M}(t) = -M(t)\dot{C}(t)M(t) - \lambda C^{\mathrm{H}}(t)\left(C(t)M(t) - I\right)$	$M_{k+1} \doteq -\tau M_k \dot{C}_k M_k - hC_k^{\mathrm{H}}(C_k M_k - I) + M_k$ $M_{k+1} \doteq -\tau M_k \dot{C}_k M_k - hC_k^{\mathrm{H}}(C_k M_k - I) + \frac{3}{2}M_k$ $-M_{k-1} + \frac{1}{2}M_{k-2}$ $M_{k+1} \doteq -\frac{42}{23}\tau M_k \dot{C}_k M_k - \frac{42}{23}hC_k^{\mathrm{H}}(C_k M_k - I)$ $+\frac{11}{23}M_k + \frac{4}{23}M_{k-1} + \frac{5}{23}M_{k-2}$ $+\frac{7}{23}M_{k-3} - \frac{4}{23}M_{k-4}$ $M_{k+1} \doteq -\frac{111}{50}\tau M_k \dot{C}_k M_k - \frac{111}{50}hC_k^{\mathrm{H}}(C_k M_k - I)$ $+\frac{51}{1000}M_k + \frac{2}{5}M_{k-1} + \frac{3}{5}M_{k-2} + \frac{1}{5}M_{k-3}$ $-\frac{7}{40}M_{k-4} - \frac{22}{125}M_{k-5} + \frac{1}{10}M_{k-6}$ $M_{k+1} \doteq -\frac{72}{31}\tau M_k \dot{C}_k M_k - \frac{72}{31}hC_k^{\mathrm{H}}(C_k M_k - I)$ $-\frac{3}{31}M_k + \frac{16}{31}M_{k-1} + \frac{24}{31}M_{k-2} + \frac{1}{31}M_{k-3}$ $-\frac{7}{31}M_{k-4} - \frac{2}{31}M_{k-5} + \frac{2}{31}M_{k-6}$
GZ model 3	$\dot{M}(t) = -M(t)\dot{C}(t)M(t) - \lambda\left(M(t)C(t) - I\right)C^{\mathrm{H}}(t)$	$M_{k+1} \doteq -\tau M_k \dot{C}_k M_k - h(M_k C_k - I)C_k^{\mathrm{H}} + M_k$ $M_{k+1} \doteq -\tau M_k \dot{C}_k M_k - h(M_k C_k - I)C_k^{\mathrm{H}} + \frac{3}{2}M_k$ $-M_{k-1} + \frac{1}{2}M_{k-2}$ $M_{k+1} \doteq -\frac{42}{23}\tau M_k \dot{C}_k M_k - \frac{42}{23}h(M_k C_k - I)C_k^{\mathrm{H}}$ $+\frac{11}{23}M_k + \frac{4}{23}M_{k-1} + \frac{5}{23}M_{k-2}$ $+\frac{7}{23}M_{k-3} - \frac{4}{23}M_{k-4}$ $M_{k+1} \doteq -\frac{111}{50}\tau M_k \dot{C}_k M_k - \frac{111}{50}h(M_k C_k - I)C_k^{\mathrm{H}}$ $+\frac{51}{1000}M_k + \frac{2}{5}M_{k-1} + \frac{3}{5}M_{k-2} + \frac{1}{5}M_{k-3}$ $-\frac{7}{40}M_{k-4} - \frac{22}{125}M_{k-5} + \frac{1}{10}M_{k-6}$ $M_{k+1} \doteq -\frac{72}{31}\tau M_k \dot{C}_k M_k - \frac{72}{31}h(M_k C_k - I)C_k^{\mathrm{H}}$ $-\frac{3}{31}M_k + \frac{16}{31}M_{k-1} + \frac{24}{31}M_{k-2} + \frac{1}{31}M_{k-3}$ $-\frac{7}{31}M_{k-4} - \frac{2}{31}M_{k-5} + \frac{2}{31}M_{k-6}$

and

$$M_{k+1} \doteq -\frac{111}{50}\tau M_k \dot{C}_k M_k - \frac{111}{50}h(M_k C_k - I)C_k^{\mathrm{H}} + \frac{51}{1000}M_k + \frac{2}{5}M_{k-1} + \frac{3}{5}M_{k-2} + \frac{1}{5}M_{k-3} - \frac{7}{40}M_{k-4} - \frac{22}{125}M_{k-5} + \frac{1}{10}M_{k-6}. \quad (20)$$

Another three discrete-time GZ models discretized by (17) are shown as follows:

$$M_{k+1} \doteq -\frac{72}{31}\tau M_k \dot{C}_k M_k - \frac{72}{31}hM_k(C_k M_k - I) - \frac{3}{31}M_k + \frac{16}{31}M_{k-1} + \frac{24}{31}M_{k-2} + \frac{1}{31}M_{k-3} - \frac{7}{31}M_{k-4} - \frac{2}{31}M_{k-5} + \frac{2}{31}M_{k-6}, \quad (21)$$

$$M_{k+1} \doteq -\frac{72}{31}\tau M_k \dot{C}_k M_k - \frac{72}{31}hC_k^{\mathrm{H}}(C_k M_k - I) - \frac{3}{31}M_k + \frac{16}{31}M_{k-1} + \frac{24}{31}M_{k-2} + \frac{1}{31}M_{k-3} - \frac{7}{31}M_{k-4} - \frac{2}{31}M_{k-5} + \frac{2}{31}M_{k-6}, \quad (22)$$

and

$$M_{k+1} \doteq -\frac{72}{31}\tau M_k \dot{C}_k M_k - \frac{72}{31}h(M_k C_k - I)C_k^{\mathrm{H}} - \frac{3}{31}M_k + \frac{16}{31}M_{k-1} + \frac{24}{31}M_{k-2} + \frac{1}{31}M_{k-3} - \frac{7}{31}M_{k-4} - \frac{2}{31}M_{k-5} + \frac{2}{31}M_{k-6}. \quad (23)$$

We name (18), (19), (20), (21), (22), and (23) as DTGZ1-IV, DTGZ2-IV, DTGZ3-IV, DTGZ1-V, DTGZ2-V, and DTGZ3-V, respectively.

Hitherto, we complete the discrete-time GZ models. Moreover, we gather them in Table I.

IV. Numerical Experiments and Results

Using different time-discretization formulas, we carry out two examples' numerical computer experiments to verify whether the above discrete GZ models are effective, and make comparisons on their efficiency.

A. First Example

In this example, the experimental object is a 3×3 real time-varying matrix, and it is described as

$$C_k = \begin{bmatrix} 5+\sin(4t_k) & 0.25\cos(4t_k) & \cos(4t_k) \\ 0.25\cos(4t_k) & 5+\sin(4t_k) & 0.25\cos(4t_k) \\ \cos(4t_k) & 0.25\cos(4t_k) & 5+\sin(4t_k) \end{bmatrix} \in \mathbb{R}^{3\times 3},$$

where $t_k = k\tau$ with $k \in \mathbb{N}$. Suppose that C_k^{-1} is the theoretical inverse of C_k. Due to the complexity of the elements of C_k^{-1}, we omit C_k^{-1} here. The initialization C_0 of C_k is set randomly (and also sufficiently close to C_0^{-1}). the sampling interval τ, the step size h, and the simulation duration are uniformly set as 10^{-3} s, 10^{-2}, and 10 s. The results of the numerical experiments are exhibited in Figs. 1 & 2. Precisely, Fig. 1(a) displays $\|M_{k+1} - C_{k+1}^{-1}\|_{\mathrm{F}}$ (i.e., solution errors) of five discrete-time models obtained from GZ model 1, i.e., correspondingly, DTGZ1-I (7), DTGZ1-II (10), DTGZ1-III (13), DTGZ1-IV (18), and DTGZ1-V (21). Fig. 1(b) and (c) show the solution errors $\|M_{k+1} - C_{k+1}^{-1}\|_{\mathrm{F}}$ of DTGZ2-I (8) through DTGZ2-V (22) and DTGZ3-I (9) through DTGZ3-V (23), respectively. Besides, Fig. 2(a) through (c) present the residual errors $\|C_{k+1}M_{k+1} - I\|_{\mathrm{F}}$ of DTGZ1-I (7) through DTGZ1-V (21), DTGZ2-I (8) through DTGZ2-V (22), and DTGZ3-I (9) through DTGZ3-V (23), respectively. As presented in Fig. 1, the numerical results substantiate that three GZ models and their corresponding discrete-time ones are effective. However, the convergence phenomena arise earlier in Fig. 1(b) & (c) than those in Fig. 1(a), and so do the phenomena in Fig. 2, which indicates the second and the third GZ models (i.e., (4) and (6)) have better performance. As mentioned in Section II before, GZ model 2 and 3 utilize GDS's strength, namely fast convergence rate.

TABLE II: Solution errors and residual errors of discrete GZ models for first example with $\tau = 10^{-3}$ s and $h = 10^{-2}$

Discrete-time model	Solution error	Residual error
DTGZ1-I (7)	5.15×10^{-5}	2.86×10^{-4}
DTGZ1-II (10)	3.12×10^{-8}	1.58×10^{-7}
DTGZ1-III (13)	5.51×10^{-10}	2.76×10^{-9}
DTGZ1-IV (18)	6.98×10^{-12}	3.52×10^{-11}
DTGZ1-V (21)	5.84×10^{-12}	2.95×10^{-12}
DTGZ2-I (8)	1.49×10^{-6}	8.15×10^{-6}
DTGZ2-II (11)	4.39×10^{-9}	2.20×10^{-8}
DTGZ2-III (14)	4.04×10^{-11}	2.03×10^{-10}
DTGZ2-IV (19)	3.65×10^{-13}	1.83×10^{-12}
DTGZ2-V (22)	3.06×10^{-13}	1.53×10^{-12}
DTGZ3-I (9)	1.49×10^{-6}	8.15×10^{-6}
DTGZ3-II (12)	4.39×10^{-9}	2.20×10^{-8}
DTGZ3-III (15)	4.04×10^{-11}	2.03×10^{-10}
DTGZ3-IV (20)	3.65×10^{-13}	1.83×10^{-12}
DTGZ3-V (23)	3.06×10^{-13}	1.53×10^{-12}

Besides, we list the values of the solution errors and residual ones synthesized by the discrete-time models in Table II. Observed from Table II, in terms of the same GZ model, the higher the precision of a time-discretization formula is, the smaller two types of errors of the obtained discrete model are. That is to say, the precision of a formula used for time discretization influences the accuracy of the obtained model. Additionally, different discrete models acquired by discretizing the same continuous GZ model with different time-discretization formulas have their own precisions associated with the formulas, which is distinct from GZ variants [17]. Moreover, when adopting the same time-discretization formula, two kinds of errors of the discrete GZ model 1 are both larger than those of the discrete GZ model 2 and 3, which illustrates that GZ model 2 (4) and 3 (6) perform better than GZ model 1 (2) again. Furthermore, it is surprising to discover that the discrete GZ model 2 and 3 possess the same accuracy when exerting the same time-discretization formula.

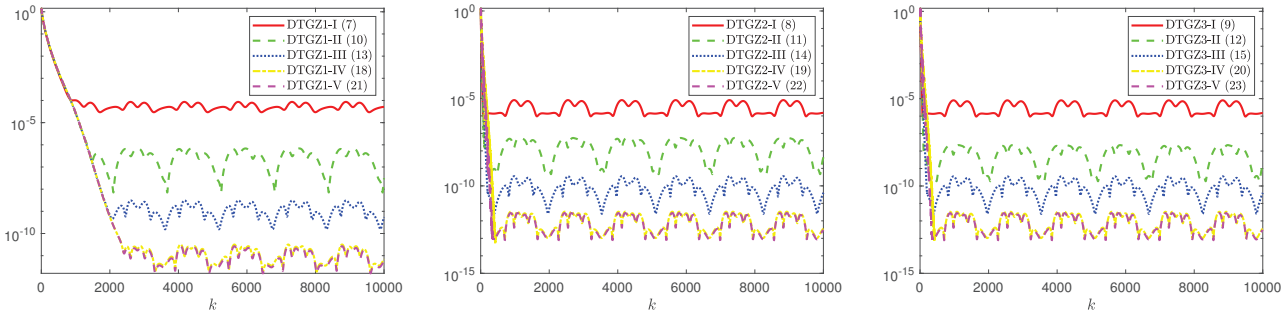

(a) (b) (c)

Fig. 1: Solution errors $\|M_{k+1} - C_{k+1}^{-1}\|_{\mathrm{F}}$ synthesized by discrete-time GZ models for first example with $\tau = 10^{-3}$ s and $h = 10^{-2}$. (a) Discrete-time GZ model 1. (b) Discrete-time GZ model 2. (c) Discrete-time GZ model 3.

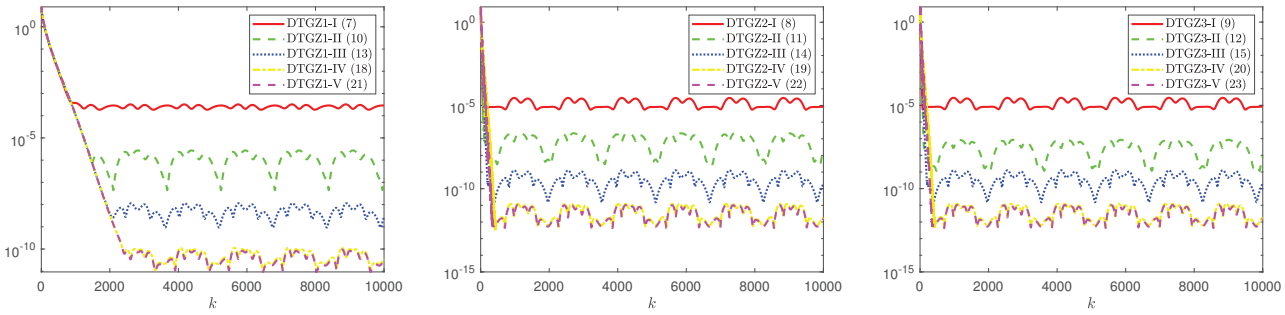

(a) (b) (c)

Fig. 2: Residual errors $\|C_{k+1}M_{k+1} - I\|_{\mathrm{F}}$ synthesized by discrete-time GZ models for first example with $\tau = 10^{-3}$ s and $h = 10^{-2}$. (a) Discrete-time GZ model 1. (b) Discrete-time GZ model 2. (c) Discrete-time GZ model 3.

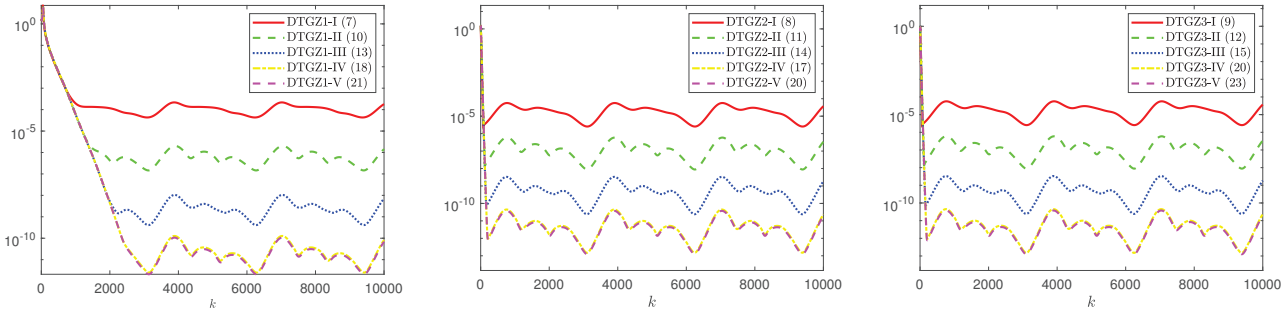

(a) (b) (c)

Fig. 3: Solution errors $\|M_{k+1} - C_{k+1}^{-1}\|_{\mathrm{F}}$ synthesized by discrete-time GZ models for second example with $\tau = 10^{-3}$ s and $h = 10^{-2}$. (a) Discrete-time GZ model 1. (b) Discrete-time GZ model 2. (c) Discrete-time GZ model 3.

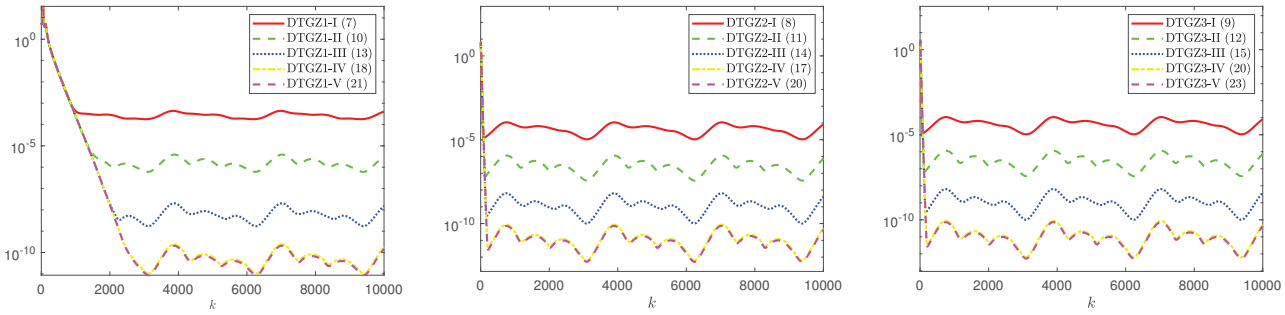

(a) (b) (c)

Fig. 4: Residual errors $\|C_{k+1}M_{k+1} - I\|_{\mathrm{F}}$ synthesized by discrete GZ models for second example with $\tau = 10^{-3}$ s and $h = 10^{-2}$. (a) Discrete-time GZ model 1. (b) Discrete-time GZ model 2. (c) Discrete-time GZ model 3.

TABLE III: Solution errors and residual errors of discrete-time GZ models for second example with $\tau = 10^{-3}$ s and $h = 10^{-2}$

Discrete-time model	Solution error	Residual error
DTGZ1-I (7)	1.81×10^{-4}	4.07×10^{-4}
DTGZ1-II (10)	1.44×10^{-6}	3.15×10^{-6}
DTGZ1-III (13)	7.05×10^{-9}	1.55×10^{-8}
DTGZ1-IV (18)	8.19×10^{-11}	1.79×10^{-10}
DTGZ1-V (21)	6.85×10^{-11}	1.50×10^{-10}
DTGZ2-I (8)	3.72×10^{-5}	8.17×10^{-5}
DTGZ2-II (11)	3.41×10^{-7}	7.46×10^{-7}
DTGZ2-III (14)	1.85×10^{-9}	4.05×10^{-9}
DTGZ2-IV (19)	2.34×10^{-11}	5.13×10^{-11}
DTGZ2-V (22)	1.96×10^{-11}	4.30×10^{-11}
DTGZ3-I (9)	3.72×10^{-5}	8.17×10^{-5}
DTGZ3-II (12)	3.41×10^{-7}	7.46×10^{-7}
DTGZ3-III (15)	1.85×10^{-9}	4.05×10^{-9}
DTGZ3-IV (20)	2.34×10^{-11}	5.13×10^{-11}
DTGZ3-V (23)	1.96×10^{-11}	4.30×10^{-11}

B. Second Example

Another experimental object is a 3×3 complex time-varying matrix, and it is described as

$$C_k = \begin{bmatrix} 3+\exp(2\mathrm{i}t_k) & -0.5\mathrm{i}\exp(-2\mathrm{i}t_k) & -\mathrm{i}\exp(-2\mathrm{i}t_k) \\ -0.5\mathrm{i}\exp(-2\mathrm{i}t_k) & 3+\exp(2\mathrm{i}t_k) & -0.5\mathrm{i}\exp(-2\mathrm{i}t_k) \\ -\mathrm{i}\exp(-2\mathrm{i}t_k) & -0.5\mathrm{i}\exp(-2\mathrm{i}t_k) & 3+\exp(2\mathrm{i}t_k) \end{bmatrix},$$

where $C_k \in \mathbb{C}^{3\times3}$. Suppose that C_k^{-1} is the theoretical inverse of C_k. Similarly, due to the complexity of the elements of C_k^{-1}, we omit it here. The initialization M_0 of M_k is set randomly too. the sampling interval τ, the step size h, and the simulation duration are also uniformly set as 10^{-3} s, 10^{-2}, and 10 s. The results are illustrated in Figs. 3 & 4 as well as Table III. Evidently, three GZ models work pretty well. What is more, the phenomena observed in the first example also appear in the second example, meaning that, from the perspective of complex time-varying matrices, the summaries made in the first example are also valid.

V. Conclusion

This paper has elaborated the design procedures of three GZ models, which secure the inverse of an interesting matrix varied with time, and discretized them by five different time-discretization formulas. Through experiments, it has been discovered that GZ model 2 depicted in (4) and GZ model 3 depicted in (6) have higher convergence accuracy and faster convergence rate, compared with GZ model 1 depicted in (2). Besides, with regard to the same time-discretization formula, the results of GZ model 2 depicted in (4) and GZ model 3 depicted in (6) are fully the same. In addition, different discrete-time GZ models have their own precisions related to the exploited time-discretization formulas. Due to space limitation, a detailed and deep review of relevant literatures has not been provided, and it may be a research direction in future.

Acknowledgment

This work is aided by the National Natural Science Foundation of China under the Grant Number 61976230, the Project Supported by Guangdong Province Universities and Colleges Pearl River Scholar Funded Scheme under the Grant Number 2018, the Key-Area Research and Development Program of Guangzhou under the Grant Number 202007030004, and the Research Fund Program of Guangdong Key Laboratory of Modern Control Technology under the Grant Number 2017B030314165.

References

[1] S. Li, S. Chen, B. Liu, Y. Li, and Y. Liang, "Decentralized kinematic control of a class of collaborative redundant manipulators via recurrent neural networks", *Neurocomputing*, vol. 91, pp. 1–10, 2012.

[2] R. H. Sturges, "Analog matrix inversion (robot kinematics)", *IEEE J. Robot. Autom.*, vol. 4, no. 2, pp. 157–162, 1988.

[3] Y. Zhang and C. Yi, *Zhang Neural Networks and Neural-Dynamic Method*. New York, NY, USA: Nova Science Publishers, 2011.

[4] B. Arnonkijpanicha, A. Hasenfussb, and B. Hammer, "Local matrix adaptation in topographic neural maps", *Neurocomputing*, vol. 74, no. 4, pp. 522–539, 2011.

[5] B. Liao and Y. Zhang, "Different complex ZFs leading to different complex ZNN models for time-varying complex generalized inverse matrices", *IEEE Trans. Neural Netw. Learn. Syst.*, vol. 25, no. 9, pp. 1621–1631, 2014.

[6] R. J. Steriti and M. A. Fiddy, "Regularized image reconstruction using SVD and a neural network method for matrix inversion", *IEEE Trans. Signal Process.*, vol. 41, no. 10, pp. 3074–3077, 1993.
[7] K. Chen, "Implicit dynamic system for online simultaneous linear equations solving", *Electron. Lett.*, vol. 49, no. 2, pp. 101–102, 2013.
[8] Y. Zhang, K. Chen, and H. Tan, "Performance analysis of gradient neural network exploited for online time-varying matrix inversion", *IEEE Trans. Automat. Contr.*, vol. 54, no. 8, pp. 1940–1945, 2009.
[9] S. Li and F. Qin, "A dynamic neural network approach for solving nonlinear inequalities defined on a graph and its application to distributed, routing-free, range-free localization of WSNs", *Neurocomputing*, vol. 117, no. 1, pp. 72–80, 2013.
[10] C. Qiao and Z. Xu, "Critical dynamics study on recurrent neural networks: Globally exponential stability", *Neurocomputing*, vol. 77, no. 1, pp. 205–211, 2012.
[11] S. Li, S. Chen, and B. Liu, "Accelerating a recurrent neural network to finite-time convergence for solving time-varying Sylvester equation by using a sign-bi-power activation function", *Neural. Process. Lett.*, vol. 37, no. 2, pp. 189–205, 2013.
[12] Y. Zhang, D. Jiang, and J. Wang, "A recurrent neural network for solving Sylvester equation with time-varying coefficients", *IEEE Trans. Neural Netw.*, vol. 13, no. 5, pp. 1053–1063, 2002.
[13] L. Xiao and Y. Zhang, "A new performance index for the repetitive motion of mobile manipulators", *IEEE Trans. Cybern.*, vol. 44, no. 2, pp. 280–292, 2014.
[14] Y. Zhang, C. Peng, W. Li, Y. Shi, and Y. Ling, "Broyden-method aided discrete ZNN solving the systems of time-varying nonlinear equations", *International Conference on Control Engineering and Communication Technology*, pp. 492–495, 2012.
[15] N. H. Getz and J. E. Marsden, "Dynamical methods for polar decomposition and inversion of matrices", *Linear. Algebra Appl.*, vol. 258, pp. 311–343, 1997.
[16] D. Wu, Y. Zhang, J. Guo, Z. Li, and L. Ming, "GMDS-ZNN model 3 and its ten-instant discrete algorithm for time-variant matrix inversion compared with other multiple-instant ones", *IEEE Access*, vol. 8, pp. 228188–228198, 2020.
[17] J. Li, G. Wu, C. Li, M. Xiao, and Y. Zhang, "GMDS-ZNN variants having errors proportional to sampling gap as compared with models 1 and 2 having higher precision", *International Conference on Systems and Informatics*, pp. 728–733, 2018.
[18] W. Tang, C. Ke, and M. Fu, "Electrically tunable magnetic configuration on vacancy-doped GaSe monolayer", *Phys. Lett. A*, vol. 382, no. 9, pp. 667–672, 2018.
[19] Y. Zhang, G. Shi, J. Li, G. Wu, and Z. Qi, "Zhang matrix found as an exception with its time-dependent pseudoinverse unsolvable by Getz-Masden dynamic system", *International Conference on Systems and Informatics*, pp. 757–762, 2018.
[20] Y. Zhang, Z. Li, Y. Ling, M. Yang, and B. Qiu, "Time-varying complex Zhang matrix (ZM) with its pseudoinverse not solvable directly by Getz-Masden (GM) dynamic system", *IEEE Symposium Series on Computational Intelligence*, pp. 519–526, 2019.
[21] Y. Zhang, L. Jin, D, Guo, Y. Yin, and Y. Chou, "Taylor-type 1-step-ahead numerical differentiation rule for first-order derivative approximation and ZNN discretization", *J. Comput. Appl. Math*, vol. 273, pp. 29–40, 2015.
[22] Y. Zhang, H. Huang, Y. Shi, J. Li, and J. Wen, "Numerical experiments and verifications of ZFD formula 4NgSFD for first-order derivative discretization and approximation", *International Conference on Machine Learning and Cybernetics*, vol. 1, pp. 87–92, 2016.
[23] Y. Zhang, X. Yang, J. Wang, J. Li, and L. He, "New formula 4IgSFD_L of Zhang finite difference for 1st-order derivative approximation with numerical experiment verification", *International Conference on Computer Science and Network Technology*, pp. 206–209, 2016.
[24] Y. Zhang, H. Huang, P. He, M. Yang, and J. Wen, "Solving ordinary differential equations by ZFD formula 4NgSFD", *Chinese Control and Decision Conference*, pp. 2888–2893, 2017.
[25] Y. Zhang, C. Li, P. He, M. Yang, and X. Yang, "New ZFD (Zhang finite difference) formula 4IgSFD_L for time-varying reciprocal and inverse computation", *Chinese Control and Decision Conference*, pp. 2894–2899, 2017.
[26] Y. Zhang, H. Xiao, J. Wang, J. Li, and P. Chen, "Discrete-time control and simulation of ship course tracking using ZD method and ZFD formula 4NgSFD", *Information Technology and Mechatronics Engineering Conference*, pp. 6–10, 2017.
[27] Y. Zhang, M. Yang, J. Li, L. He, and S. Wu, "ZFD formula 4IgSFD_Y applied to future minimization", *Phys. Lett. A*, vol. 381, no. 19, pp. 1677–1681, 2017.
[28] Y. Zhang, J. Zhang, Y. Ding, H. Gong, and J. Li, "Euler-precision formula ZD3NgyP_Z applied to discrete control simulation of agitation tank", *Chinese Automation Congress*, pp. 363–368, 2017.
[29] Y. Zhang, M. Zhu, C. Hu, J. Li, and M. Yang, "Euler-precision general-form of Zhang et al discretization (ZeaD) formulas, derivation, and numerical experiments", *Chinese Control and Decision Conference*, pp. 6262–6267, 2018.
[30] J. Stoer and R. Bulirsch, *Introduction to Numerical Analysis*. New York, NY, USA: Springer, 2002.
[31] J. H. Mathews and K. D. Fink, *Numerical Methods Using MATLAB*. Upper Saddle River, NJ, USA: Pearson Prentice Hall, 2004.
[32] Y. Zhang, H. Gong, M. Yang, J. Li, and X. Yang, "Stepsize range and optimal value for Taylor-Zhang discretization formula applied to zeroing neurodynamics illustrated via future equality-constrained quadratic programming", *IEEE Trans. Neural Netw. Learn. Syst.*, vol. 30, no. 4, pp. 959–966, 2019.
[33] Y. Zhang, X. Liu, J. Guo, Z. Yin, and H. Hu, "Discrete control and simulation of zero-vibration hovering of sling-load helicopter using six-instant and seven-instant ZeaD formulas", *Chinese Control Conference*, pp. 618–624, 2019.
[34] B. Qiu and Y. Zhang, "Two new discrete-time neurodynamic algorithms applied to online future matrix inversion with non-singular or sometimes-singular coefficient", *IEEE Trans. Cybern.*, vol. 49, no. 6, pp. 2034–2045, 2018.
[35] J. Chen, J. Guo, and Y. Zhang, "General ten-instant DTDMSR model for dynamic matrix square root finding", *Cybern. Syst.*, vol. 52, no. 1, pp. 127–143, 2021.
[36] B. Qiu, J. Guo, X. Li, Z. Zhang, and Y. Zhang, "Discrete-time advanced zeroing neurodynamic algorithm applied to future equality-constrained nonlinear optimization with various noises", *IEEE Trans. Cybern.*, pp. 1–14, doi: 10.1109/TCYB.2020.3009110, 2020.